

A THEORY FOR THE RADIUS OF THE TRANSITING GIANT PLANET HD 209458B

ADAM BURROWS¹, D. SUDARSKY¹ AND W.B. HUBBARD²*Accepted to Ap.J.*

ABSTRACT

Using a full frequency-dependent atmosphere code that can incorporate irradiation by a central primary star, we calculate self-consistent boundary conditions for the evolution of the radius of the transiting planet HD 209458b. Using a well-tested extrasolar giant planet evolutionary code, we then calculate the behavior of this planet’s radius with age. The measured radius is in fact a transit radius that resides high in HD 209458b’s inflated atmosphere: Using our derived atmospheric and interior structures, we find that irradiation plus the proper interpretation of the transit radius can yield a theoretical radius that is within the measured error bars. We conclude that if HD 209458b’s true transit radius is at the lower end of the measured range, an extra source of core heating power is not necessary to explain the transit observations.

Subject headings: stars: individual (HD209458)—(stars:) planetary systems—planets and satellites: general

1. INTRODUCTION

These past seven years have seen the number of known extrasolar giant planets (EGPs) grow from 1 in 1995 (Mayor and Queloz 1995) to more than 100 today.³ The wide variety in their projected masses ($M_p \sin(i)$), orbital distances (a), and eccentricities continues to challenge theories of EGP birth, evolution, and abundance. However, as of this writing, only two EGPs (HD 209458b and OGLE-TR-56b) are claimed to transit their primaries and of the two HD 209458b is by far the best studied. The second transiting EGP, OGLE-TR-56b, has only recently been suggested as such (Konacki et al. 2003) and, at a distance of ~ 1500 parsecs, even if the detection is verified, its light curve and radial-velocity measurements are not yet competitive with those for HD 209458b. Since HD 209458’s stellar reflex motion has been accurately measured, and its transit light curve has been measured using HST/STIS to ~ 100 -micromagnitude precision (Brown et al. 2001), it is an ideal testbed for the theory of irradiated EGPs, their evolution, structure, and atmospheres. The transit of the F8V/G0V star HD 209458 lasts ~ 3 hours (out of a total period of 3.524738 days) and has an average photometric depth of $\sim 1.6\%$ in the optical. Its ingress and egress phases each last ~ 25 minutes (Henry et al. 2000; Charbonneau et al. 2000; Brown et al. 2001). Using the complementary radial-velocity data (e.g., Henry et al. 2000), good estimates for the planet’s mass, orbital distance, and orbital inclination are $\sim 0.69 M_J$, ~ 0.045 AU, and $\sim 86^\circ$, respectively. Such proximity makes HD 209458b the quintessential “roaster” (Sudarsky, Burrows, and Pinto 2000; Hubbard et al. 2001; Sudarsky, Burrows, and Hubeny 2002). Of course, the depth of the transit light curve can be used to derive the planet’s radius (§2). It is the simultaneous availability of both a radius and a mass (together with

an age estimate for the system from stellar evolution theory and a luminosity estimate for the star from its parallax) that makes this system especially useful to theorists. Moreover, Charbonneau et al. (2002) have recently binned their HST/STIS data to derive a wavelength dependence for HD 209458b’s transit radius. In this way, they have inferred the presence of neutral sodium atoms (Seager and Sasselov 2000; Hubbard et al. 2001) and, hence, have made the first measurement, however indirect, of the composition of the atmosphere of an extrasolar planet.

Importantly, the measured radius is a transit radius at a given wavelength, or range of wavelengths. It is not the canonical planetary radius at a “1-bar” pressure level (Lindal et al. 1981; Hubbard et al. 2001). As such, the measured radius is the impact parameter of the transiting planet at which the optical depth to its primary’s light along a chord parallel to the star-planet line of centers is ~ 1 . This is not the optical depth in the radial direction, nor is it associated with the radius at the radiative-convective boundary. Hence, since the pressure level to which the transit beam is probing near the planet’s terminator is close to 1 millibar (Fortney et al. 2003), there are many pressure scale heights (~ 10) between the measured transit radius and both the radiative-convective boundary (≥ 1000 bars) and the “1-bar” radius.⁴ Furthermore, exterior to the radiative-convective boundary, the entropy is an increasing function of radius. One consequence of this fact is significant radial inflation vis à vis a constant entropy atmosphere. The upshot of both these effects is an increase of $\sim 0.1 R_J$ ($\sim 10\%$) in the theoretical radius.

Including the “thickness of the atmosphere” could change recent interpretations of the radius of HD 209458b. Guillot and Showman (2002), Baraffe et al. (2002, 2003), and Bodenheimer et al. (2000, 2003) all have difficulty fit-

¹ Department of Astronomy and Steward Observatory, The University of Arizona, Tucson, AZ 85721; burrows@zenith.as.arizona.edu, sudarsky@as.arizona.edu

² Department of Planetary Sciences, Lunar and Planetary Laboratory, The University of Arizona, Tucson, AZ 85721; hubbard@lpl.arizona.edu

³ see J. Schneider’s Extrasolar Planet Encyclopaedia at <http://www.obspm.fr/encycl/encycl.html> for a current tally, with ancillary stellar data.

⁴ If, as implied in Barman et al. (2002), the transit radius is at pressures well below the 1 millibar level then the multiple-pressure-scale-height effect we identify here would be even larger.

ting HD 209458b’s radius without an extra heat source. Guillot and Showman posit the dissipation at depth of mechanical energy generated by the stellar flux at altitude. Bodenheimer et al. invoke tidal heating or the presence of an additional planetary companion in near resonance to create the “Io” heating effect. However, we find that self-consistently calculating irradiated atmospheres and the irradiated planet’s structural and thermal evolution and assuming that the lower end of the range of the measured transit radius obtains, we can fit the observations without an extra source of heat. Our calculations also self-consistently and implicitly derive a Bond albedo, generally assumed by others as an input.

In §2, we describe and discuss the measurements of HD 209458b’s transit radius. This is followed in §3 by a brief review of previous theoretical calculations of the radii of irradiated EGPs. In §4, we summarize the computational procedures we employ in this paper and discuss the various strengths and weaknesses of our approach and in §5 we present our theoretical results for the radius of HD 209458b, as well as its temporal evolution. This section contains the major conclusions of our study and includes in Fig. 2 what we think is a favorable comparison between theory and measurement. We wrap up in §6 with general remarks and caveats.

2. THE MEASURED PLANETARY RADIUS

Photometric light curve measurements of the relative transit depth of the HD 209458 system from both the ground (Henry et al. 2000; Charbonneau et al. 2000) and from space (HST/STIS: Brown et al. 2001) have provided direct estimates of the ratio of the radii of the planet and star. Mandel and Agol (2002) conclude that this ratio can be obtained from the data to relatively high precision ($R_p/R_* = 0.1207 \pm 0.0003$). Seager and Mallén-Ornelas (2003) suggest that future transit measurements alone, done with dense time sampling and the best photometric precision attainable from the ground, can yield the individual radii themselves. However, currently, estimates of the radius of the planet HD 209458b require estimates of the star’s radius and this requires both a fit to stellar evolution theory and a good parallax.⁵ As a result, ambiguities in the stellar radius translate into uncertainties in the inferred planetary radius. Mazeh et al. (2000) conclude from $\log(g)/T_{\text{eff}}$ spectral-line fits and $M_V/(B - V)$ photometric fits that $M_* = 1.1 \pm 0.1 M_\odot$, $R_* = 1.2 \pm 0.1 R_\odot$, $T_{\text{eff}} \sim 6000$ K, $[\text{Fe}/\text{H}] \sim 0.0$, and $t = 5.5 \pm 1.5$ Gyr. From these data they derive a radius for HD 209458b of $1.40 \pm 0.17 R_J$, where the error bars are one-sigma and $R_J = 7.149 \times 10^9$ cm. Similarly, Cody and Sasselov (2002) derive $R_* = 1.18 R_\odot$ and $M_* = 1.06 M_\odot$, with one-sigma error bars of $\sim 10\%$. The resultant planetary radius is $R_p = 1.42^{+0.10}_{-0.13} R_J$, where in this case the error bars in the planet radius do not include the errors in the stellar radius; Cody and Sasselov assume in deriving this estimate that the stellar radius is fixed at $1.18 R_\odot$. They also derive a best-fit age of ~ 5.2 Gyrs ($\pm 10\%$), but second the age range quoted in Mazeh et al. (2000).

Hence, to obtain a reliable stellar radius (given a parallax), one is obliged to derive the stellar metallicity, age, mass, and helium fraction simultaneously. This procedure

perforce introduces ambiguities into the estimate of the planetary radius. In particular, if Cody and Sasselov were to use for the star’s radius a value of $1.10 R_\odot$ (within their quoted errors), they would obtain a planetary radius of $1.32^{+0.09}_{-0.11} R_J$. Hence, their one-sigma lower bound would be $1.21 R_J$. At $R_* = 1.18 R_\odot$, their one-sigma lower bound is $1.29 R_J$. Similar arguments can be marshalled in the context of the Brown et al. (2001) and Mazeh et al. (2000) planet radius estimates. As a result, it is not far-fetched to conclude that HD 209458b’s transit radius in the optical could be as small as $\sim 1.2 R_J$. While we are not completely convinced that this is the correct value, it is nevertheless useful to explore the theoretical consequences of such a possibility. Given an age range for the HD 209458 system and a radius range for the planet, theories for the irradiated planet’s evolutionary trajectory in age-radius space can be compared with observations to derive physical constraints on the nature of this irradiated planet and its atmosphere.

3. PREVIOUS THEORIES FOR THE RADII OF IRRADIATED GIANT PLANETS

The modern theory of the radii of irradiated EGPs begins with the paper of Guillot et al. (1996). This paper focussed on 51 Pegasi b, but 1) predicted that irradiation due to proximity to a central primary would result in super-Jovian radii, 2) distinguished clearly between the radii of hydrogen-rich and metal-rich giants (in the tradition of Zepolsky and Salpeter 1969), and 3) suggested that lower-mass irradiated EGPs will be larger, all else being equal. However, these calculations were performed using an irradiation-modified version of atmospheric boundary conditions (needed for the evolutionary calculations) appropriate for isolated giants (Burrows et al. 1995; Burrows et al. 1997) and employed an ad hoc Bond albedo. The latter determines the absorption and heating efficiency of stellar light. A fully consistent spectrum and atmosphere calculation was not attempted. Hence, while the results were qualitatively valid, the actual radius-age trajectories obtained were ambiguous. In addition, very large radii ($1.4\text{--}1.8 R_J$) seemed plausible for older EGPs (> 1 Gyr).

In the first year of the HD 209458b campaign, Burrows et al. (2000) employed similar boundary algorithms and Bond albedo ansätze to fit HD 209458b’s measured transit radius. They concluded that the planet could not be as large as measured unless it had migrated in early in its life before it had had time to cool and shrink appreciably. They showed that once an EGP achieves mere Jovian proportions it cannot be inflated enough to conform to the new transit radius measurements. While we concur with this general conclusion, we disagree with the magnitude of the discrepancy that late migration would have created. If, as we suggest in §2, HD 209458b’s transit radius can be as small as $\sim 1.2 R_J$, we now find that the discrepancy in the radius would be $\sim 0.1 R_J$, not $\sim 0.3 R_J$, as implied in Burrows et al. (2000). This is still significant, but less so. This modified conclusion is a consequence of our better and more consistent boundary conditions and the use of a state-of-the-art, frequency-dependent stellar atmosphere code that can accurately handle insolation (§4,§5).

⁵ The Hipparcos distance to the star HD 209458 is 47.3 parsecs, with an error of $\sim 5\%$ (Perryman 1997).

Recently, Guillot and Showman (2002), using a modified version of the Guillot et al. (1996) boundary conditions, have questioned the larger radii derived in Guillot et al. (1996) and Burrows et al. (2000). They conclude that HD 209458b’s radius cannot be explained without an extra heat source and they speculate that this might be due to the degradation at depth of gravity waves generated in the upper atmosphere by a fraction of the stellar flux. However, in order to obtain boundary conditions for their new irradiated-planet evolutionary calculations (their “cold” case, without an extra heat source), they modify the atmospheric temperature/pressure profiles of isolated models (Burrows et al. 1997) by shifting the temperature at 3 bars by a somewhat arbitrary 1000 Kelvin. They suggest that this procedure mimics the effect of the thick radiative zones of close-in EGPs, through which stellar light can not penetrate to heat the convective interior. While no attempt is made to construct self-consistent atmospheres that incorporate actual stellar and planetary spectra, this procedure does qualitatively capture the expected differences in T/P profiles between distant Jovian planets and nearby roasters at the same gravity and interior entropy. The result is an HD 209458b model with a radius no greater than $\sim 1.1 R_J$. Guillot and Showman (2002) have a discussion of the possible differences between day-side and night-side cooling (see §4), but do not provide definitive quantitative guidance concerning this important, and still open, issue.

The results of Bodenheimer, Lin, and Mardling (2001) and Bodenheimer, Laughlin, and Lin (2003), who assume a Bond albedo and that the atmospheric temperature at $\tau_{\text{Rosseland}} = 2/3$ is equal to T_{eff} , are quantitatively similar to those of Guillot and Showman (2002) and they explore the possible effects of heating by tidal circularization and forcing by a second planet or of the explicit presence or absence of a heavy-element core. However, recently, in parallel with the present work, Baraffe et al. (2002, 2003) have begun to incorporate more realistic atmospheric boundary conditions into HD 209458b studies using a frequency-dependent atmosphere code. Nevertheless, they too obtain smaller radii than found in the Guillot et al. (1996) and Burrows et al. (2000) studies and, as a consequence, also evoke an another source of heat to explain the measured transit radius.

It is the thesis of this paper that a combination of the proper interpretation of the transit radius (§1) and a lower measured value of that radius (still within the error bars, §2) can be shown to be in accord with consistent and frequency-dependent atmosphere and evolutionary calculations, without an additional source of heat. These calculations do not use an ad hoc Bond albedo and do use a realistic G0 V irradiation spectrum. However, the completeness of our theory as an explanation for HD 209458b’s transit radius hinges upon the assumption that the true radius resides at the lower end of its measured range. We now turn to a description of our computational procedures.

4. COMPUTATIONAL METHODS AND ASSUMPTIONS

At the low effective temperatures achieved by brown dwarfs and EGPs, boundary conditions for evolutionary calculations must incorporate realistic atmospheres (Burrows et al. 1997; Allard et al. 1997). The traditional

method of setting the effective temperature equal to the temperature at a Rosseland mean optical depth of 2/3 does not really provide the T/P profile in the atmosphere and can lead to errors in T_{eff} of hundreds of Kelvin. Hence, for isolated objects with cold molecular atmospheres, we calculate a grid of detailed T/P profiles and spectra at various T_{eff} s and gravities (g). These atmospheres penetrate deeply into the convective core. In this way, we determine the relationship between the core entropy (S), T_{eff} , and g (Hubbard 1977). Since the core contains the mass and the heat, while the thin atmosphere is the valve that regulates radiative losses, interpolating in this pre-calculated S - T_{eff} - g grid at each timestep in an evolutionary calculation assures accuracy and self-consistency.

However, when an EGP is being irradiated by a primary star, the above procedure must be modified to include the outer stellar flux in the spectrum/atmosphere calculation that yields the corresponding S - T_{eff} - g relationship. This must be done for a given external stellar flux and spectrum, which in turn depends upon the stellar luminosity spectrum and the orbital distance of the EGP. Therefore, we use the Discontinuous Finite Element (DFE) variant of the spectral code TLUSTY (Hubeny 1988; Hubeny and Lanz 1995) that we have developed for EGP and brown dwarf atmospheres (Sudarsky, Burrows, and Hubeny 2002) to calculate a new S - T_{eff} - g grid under the irradiation regime of HD 209458b. This grid is tailor-made for the luminosity and spectrum of HD 209458 at a distance of 0.045 AU. For the stellar spectrum, we employ a theoretical G0 V spectrum of Kurucz (1994) and we assume that the orbital distance, stellar luminosity, and stellar spectrum are all constant during the EGP’s evolution. (Hence, we ignore the “faint young sun” problem.)

The procedure is straightforward. For a given inner flux boundary condition (represented by T_{eff} , where σT_{eff}^4 is the interior core flux of the EGP) and a given gravity g , we calculate the atmospheric T/P profile, including the irradiation. Using mixing-length theory, the atmosphere is continued deep into the convective region. The radiative-convective boundary may be at pressures of ~ 10 bars (for younger ages) to ~ 4000 bars (for older ages). The entropy of the core (S) is now known for a given interior heat flux (parametrized by T_{eff}) and gravity (g). After the table in S , T_{eff} (internal flux), and g is generated, it is inverted to obtain the more useful relationship $T_{\text{eff}}(S, g)$ for the interior flux. This is the function used to advance the evolutionary calculations for HD 209458b, using a state-of-the-art equation of state (Saumon, Chabrier, and Van Horn 1995) and evolutionary code (Burrows et al. 1997). Note that since an EGP core is convective the radius of the radiative-convective boundary for a given mass EGP (e.g., $0.69 M_J$) is a function of S and g alone. Implicit in this procedure is an albedo, which therefore does not have to be assumed, as well as an emergent planetary spectrum and a T/P profile to pressures below a microbar. Since we calculate the atmospheric profile, we can automatically include the multiple-scale-height effect described in §1 in our calculation of the transit radius.

We have explored the effects on the resultant EGP transit radius of variations in the helium fraction (Y_{He}), of the presence or absence of clouds in the upper atmosphere (Sudarsky, Burrows, and Hubeny 2002), of the possible

presence of a rocky core, and of changes in the opacities in the deep atmosphere (e.g., due to the presence or absence of TiO/VO). Note with the latter that our motivation for varying the opacities in this manner is not to suggest that TiO or VO may not be present (we certainly think they are), but to explore thereby the dependence on the radius evolution of large changes in the opacities at depth. Increasing Y_{He} from 0.25 or 0.28 to 0.30 can mimic the effect of a metal-rich “rock” core or envelope and slightly shrink the object (Zapolsky and Salpeter 1969; Guillot and Showman 2002). For instance, we have calculated that for an EGP with a mass of $0.69 M_J$ replacing a one-Earth-mass heavy-element core by one containing 11 Earth masses can shrink the planet’s radius by 3-4%. This amounts to approximately -350 kilometers per Earth mass. An increase in the core mass by 10 Earth masses is comparable to the effect of increasing Y_{He} by ~ 0.02 units. The models plotted in Figs. 1 and 2 do not incorporate a rocky core, though some of the models assume a high Y_{He} to mimic its presence. However, there are two major issues that in the final analysis will need to be addressed in detail before a definitive answer is derived. For the time being, they must be finessed and have been finessed in all previous theoretical studies. The first is the fact that the planet is spherical, while the insulating stellar flux is a bundle of parallel beams. This results in a flux whose angle of incidence is a function of latitude. At the sub-stellar point the flux is a maximum, while it decreases as the terminator is approached. We have introduced the flux parameter f which accounts in approximate fashion for the variation in incident flux with latitude when using a planar atmosphere code such as we employ. Hence, a value of $f = 1/2$ is a reasonable average and is our baseline value, but we have explored the consequences of the bounding values $f = 1.0$ (appropriate for the sub-stellar point) and $f = 1/4$.

The second major issue is the day-night cooling difference. The gravity and interior entropy are the same for the day and the night sides of HD 209458b. For a synchronously rotating planet such as HD 209458b, the higher core entropies needed to explain a large measured radius imply higher internal fluxes on a night side if the day and the night atmospheres are not coupled (Guillot and Showman 2002). As described in Burrows et al. (2000), the day side core flux is quite suppressed by the flattening of the temperature gradient and the thickening of the radiative zone due to irradiation. However, Showman and Guillot (2002), Menou et al. (2002), and Cho et al. (2003) have recently demonstrated that strong atmospheric circulation currents that advect heat from the day to the night side at a wide range of pressure levels are expected in HD 209458b. Showman and Guillot (2002) estimate that below pressures of ~ 1 bar the night-side cooling of the air can be quicker than the time it takes the winds to traverse the night side, but that at higher pressures the cooling timescale is far longer. Importantly, the radiative-convective boundary in HD 209458b is deep in the planet, at pressures above 1000 bars. We take this to mean that due to the coupling of the day and the night sides via strong winds at depth, the temperature-pressure profiles at the convective boundary on both sides are similar (A. Showman, private communication). This implies that HD 209458b’s core cooling rate is roughly the same in both hemispheres. This is similar to

the case of Jupiter, where the interior flux is latitude- and longitude-independent, despite solar irradiation. Clearly, a full three-dimensional radiation/hydrodynamic study or Global-Climate-Model (GCM) is necessary to resolve this thorny issue definitively, but in the interim we assume in this paper that the interiors on the day and night sides cool at the same rate.

In calculating our T/P profiles, we assume a constant g . Since g in fact decreases slightly from the bottom to the top of HD 209458b’s extended atmosphere, the thicknesses of our calculated atmospheres are slightly underestimated. Furthermore, winds carrying gas from the day side to the night side (and vice versa) should experience temperature changes at altitude that might alter the composition and cloud profiles. Since a transit observation probes the day-night terminator, such variations could affect the character of the transit itself. However, for this study, we ignore this potential complication. We use the opacity library described in Sudarsky, Burrows, and Hubeny (2002) and 5000 frequency points from 0.4 to 300 μm in calculating the T/P profiles.

5. RESULTS: R_p VERSUS AGE

Figure 1 portrays temperature-pressure profiles at various ages along the solid model trajectory plotted in Fig. 2 with $f = 0.5$, $Y_{He} = 0.30$, and without TiO/VO opacities. We plot the T/P profiles for this model only as one example among many. The positions of the radiative-convective boundaries are indicated with large dots and each profile is for a specific time (and T_{eff}) during the evolution. The pronounced inflection in the curves is predominantly a result of the near balance at some depth between countervailing incident and internal fluxes, but changes in the opacity profiles also play a role. Nevertheless, such inflections are generic features of consistent calculations of irradiated atmospheres and affect the mapping between T_{eff} , S , and g used in evolutionary calculations. As is indicated on Fig. 1, the T_{eff} for this model at 7.5 Gyr is near ~ 62 K, which implies a $\sim 65\%$ lower internal flux than obtained for the isolated (I) model. For the isolated model at 7.5 Gyr, T_{eff} is ~ 82 K. The large contrast between these low T_{eff} s and the high atmospheric temperatures (1000-2000 K) seen in Fig. 1 for an irradiated object may seem counterintuitive, until one realizes that T_{eff} is the interior “flux temperature” from which the core luminosity is derived. Evolution over time and the stanching of heat loss by the hot atmospheric thermal blanket result in flux temperatures for irradiated objects that are smaller than, but of the same order as, those for isolated or orbitally distant EGPs (Burrows et al. 2000).

Figure 2 compares the transit radius data summarized in §2 with various representative radius-age trajectories calculated in this paper. The theoretical ages start at 10^8 years and the radii are in Jovian units ($1 R_J \equiv 7.149 \times 10^4$ km). As described in §1, the radius at the 1.0 millibar level is taken to be the relevant radius (Fortney et al. 2003). In this way, the thickness of the atmosphere, which thereby contributes $0.08 R_J$ to $0.13 R_J$ to the total radius, is incorporated into the theoretical numbers. The $1-\sigma$ radius ranges inferred by Mazeh et al. (2000, red), Brown et al. (2001, green), and Cody and Sasselov (2002, gold) are plotted; for all observational estimates the age is as-

sumed to be bracketed by 4 and 7 Gyr. For the Cody and Sasselov (2002) data, two boxes, one assuming a stellar radius of $1.18 R_{\odot}$ (solid gold) and the other assuming a stellar radius of $1.1 R_{\odot}$ (dashed gold), are provided. The red curve adjacent to an **I** is the corresponding trajectory for an isolated EGP with a helium fraction of 0.28. As one can clearly see, the difference between the **I** trajectory and the irradiated trajectories is approximately $\sim 0.2 R_J$.

The theoretical irradiated trajectories are all shown in Fig. 2 in blue. The solid curve is for $f = 0.5$, $Y_{He} = 0.30$, does not include TiO and VO at depth, and does not have clouds (see Fig. 1). The short dashed curve is similar, but includes both TiO/VO at depth and a forsterite cloud at altitude (Fortney et al. 2003). The dotted curve is for $f = 1.0$, but otherwise has the same parameters as the solid curve, and the long-dashed curve has no TiO or VO at depth, no cloud, and a helium fraction of 0.25. The presence or absence of TiO/VO is meant to gauge the effect of significant changes in opacity at higher pressures and temperatures. We see that the effect of altering this opacity, while discernable, is not large. This representative model set illustrates and quantifies several clear systematic trends. The first is that the radius is a decreasing function of increasing Y_{He} (or metallicity). A larger Y_{He} might mimic the effect of a rocky core (Guillot and Showman 2002). The second is that a larger f yields a larger radius. Intense irradiation inflates the atmosphere and at a given epoch results in interiors with slightly higher entropies. The third is that the extra opacity effect of a cloud seems to decrease the radius. However, this last trend is actually a bit misleading, since the presence of a cloud also puts the transit radius at lower pressure levels, thereby increasing the measured radius. The two effects roughly cancel. For none of the models shown is there an extra source of heating power. The finite thickness of the atmosphere and the low pressure level of the actual transit radius account for $\sim 0.1 R_J$ of our theoretical radii and are the major reasons we differ from the theories of Guillot and Showman (2002), Bodenheimer, Lin, and Mardling (2001), and Bodenheimer, Laughlin, and Lin (2003). Baraffe et al. (2003) do account for the finite thickness of the atmosphere, but their estimated thickness is about half the thickness that we obtain here. Moreover, details of the atmospheric boundary condition govern the core entropy, and, hence, the overall size of the planet. This dependence can also lead to dispersion in theoretical estimates of the planet's size.

The general proximity of the sheaf of models on Fig. 2 to the $1\text{-}\sigma$ lower bounds of the measured radius is what motivates us to suggest that an additional heat source may not be necessary to explain the HD 209458b radius measurements. However, the effective Y_{He} or f and the role of day-night thermal coupling by winds are not yet sufficiently well constrained to pinpoint the theoretical radius of the $0.69\text{-}M_J$ EGP, HD 209459b, to better than $\sim 0.05\text{-}0.1 R_J$. Note that we obtain a theoretical upper bound to the transit radius of HD 209458b at 4.0 Gyr of $\sim 1.3 R_J$ if $Y_{He} = 0.25$, $f=1.0$, there is no rocky core, and the TiO/VO opacity is suppressed. Radii greater than this for

HD 209458b will be difficult to explain without significant alterations in the physics or chemistry and/or without an extra source of internal power.

6. CONCLUSIONS

We have calculated consistent T/P profiles for various models of an irradiated HD 209458b. These profiles penetrate deeply into its inner convective zone and have been used to derive realistic boundary conditions for evolutionary models of its transit radius. The latter has been pegged to the ~ 1 -millibar pressure level inferred in the work of Fortney et al. (2003) and Hubbard et al. (2001) and accounts for $\sim 10\%$ of the total radius. We find that irradiation and the proper interpretation of the measured radius as the transit radius alone can explain HD 209458b's observed radius, without invoking an additional source of heating, if its true transit radius is at the lower end of the measured range.

Major caveats and uncertainties remain and include the actual effect of heat transport by winds from the day to the night sides, the possible presence of a rocky core, the actual helium fraction, and the true effective insolation parameter f . To resolve most of these issues will require multi-dimensional modeling with realistic radiative/convective transport. If the actual helium fraction is greater than ~ 0.28 , then a rocky core much larger than ~ 15 Earth masses may be difficult to accommodate. If better measurements of the transit radius indeed yield large radii for HD 209458b at or above $\sim 1.40 R_J$, then our interpretation is not tenable. However, if radii closer to the current lower error bars are proven to obtain, we would conclude that the theory of the structure of irradiated EGPs is in hand and well poised to interpret the new transiting EGPs anticipated to be discovered in the next few years.

Curiously, the preliminary radius for OGLE-TR-56b obtained by Konacki et al. 2003) is only $1.3 \pm 0.15 R_J$, despite its extreme proximity (~ 0.023 AU) to its central sun-like star. Having a mass ($\sim 0.9 M_J$) similar to that of HD209458b ($\sim 0.69 M_J$), one might have expected the radius of HD209459b (at an orbital distance of ~ 0.045 AU) to have been smaller, not larger, than that of OGLE-TR-56b. This could suggest that our theory for irradiated EGPs is basically correct, and that additional heat sources are not the norm, but that the transit radius of HD209458b is anomalously large, perhaps because of the special circumstance of a companion (as suggested by Bodenheimer et al.). With a collection of transits, supplemented with good radial-velocity data, and a family of radius-mass pairs for different irradiation regimes, we will be able to check this hypothesis, as well as our general theory for irradiated planet transit radii. Such a family will be a major boon to the emerging study of extrasolar giant planets.

We would like to thank Ivan Hubeny, Dimitar Sasselov, Adam Showman, Jonathan Lunine, Drew Milsom, Jonathan Fortney, Curtis Cooper, and Christopher Sharp for insightful discussions during the course of this work. This work was supported in part by NASA grants NAG5-10760 and NAG5-10629.

REFERENCES

- Allard, F., Hauschildt, P. H., Alexander, D. R. & Starrfield, S. 1997, *ARA&A*, 35, 137
- Baraffe, I. et al. 2002, to be published in "Scientific Frontiers in Research on Extrasolar Planets," ASP Conf. Series vol. 28, eds. D. Deming and S. Seager.
- Baraffe, I., Chabrier, G., Barman, T.S., Allard, F., and Hauschildt, P.H. 2003, *Astron. Astrophys.* 402, 701
- Barman, T.S., Hauschildt, P.H., Schweitzer, A., Stancil, P.C., Baron, E., and Allard, F. 2002, *ApJ*, 569, L51
- Bodenheimer, P., Lin, D.N.C., Mardling, R.A. 2001, *ApJ*, 548, 466
- Bodenheimer, P., Laughlin, G., and Lin, D.N.C. 2003, *astro-ph/0303541*
- Brown, T. M., Charbonneau, D., Gilliland, R.L., Noyes, R.W., and Burrows, A. 2001, *ApJ*, 552, 699
- Burrows, A., Saumon, D., Guillot, T., Hubbard, W.B., & Lunine, J.I. 1995, *Nature*, 375, 299
- Burrows, A., Marley, M., Hubbard, W. B., Lunine, J. I., Guillot, T., Saumon, D., Freedman, R., Sudarsky, D., & Sharp, C. 1997, *ApJ*, 491, 856
- Burrows, A., Guillot, T., Hubbard, W. B., Marley, M. S., Saumon, D., Lunine, J. I., & Sudarsky, D. 2000, 534, 97
- Charbonneau, D., Brown, T. M., Latham, D. W., & Mayor, M. 2000, *ApJ*, 529, L45
- Charbonneau, D., Brown, T. M., Noyes, R. W., & Gilliland, R. L. 2002, *ApJ*, 568, 377
- Cho, J. Y-K., Menou, K., Hansen, B. M. S., & Seager, S. 2003, *ApJ*, 587, L113
- Cody, A. M. & Sasselov, D. D. 2002, *ApJ*, 569, 451
- Fortney, J.J., Sudarsky, D., Hubeny, I., Cooper, C.S., Hubbard, W.B., Burrows, A., and Lunine, J.I. 2003, accepted to *ApJ*
- Goukenleuque, C., Bezar, B., Joguet, B., Lellouch, E., & Freedman, R. 2000, *Icarus*, 143, 308
- Guillot, T., Burrows, A., Hubbard, W. B., Lunine, J. I., & Saumon, D. 1996, *ApJ*, 459, 35
- Guillot, T. & Showman, A. P. 2002, *A&A*, 385, 156
- Henry, G., Marcy, G. W., Butler, R. P., & Vogt, S. S. 2000, *ApJ*, 529, L41
- Hubbard, W.B. 1977, *Icarus*, 30, 305
- Hubbard, W. B., Fortney, J. F., Lunine, J. I., Burrows, A., Sudarsky, D., & Pinto, P. A. 2001, *ApJ*, 560, 413
- Hubeny, I. 1988, *Computer Physics Comm.*, 52, 103
- Hubeny, I. and Lanz, T. 1995, *ApJ*, 439, 875
- Konacki, M., Torres, G., Jha, S., and Sasselov, D. 2003, *Nature*, 421, 507
- Kurucz, R. 1994, *Kurucz CD-ROM No. 19*, (Cambridge: Smithsonian Astrophysical Observatory)
- Lindal, G. F., Wood, G. E., Levy, G. S., Anderson, J. D., Sweetnam, D. N., Hotz, H. B., Buckles, B. J., Holmes, D. P., Doms, P. E., Eshleman, V. R., Tyler, G. L., and Croft, T. A. 1981, *J. Geophys. Res.*, 86, 8721
- Mandel, K. and Agol, E. 2002, *ApJ*, 580, L171
- Marley, M. S., Gelino, C., Stephens, D., Lunine J. I., & Freedman, R. 1999, *ApJ*, 513, L879
- Mayor, M. & Queloz, D. 1995, *Nature*, 378, 355
- Mazeh, T., Naef, D., Torres, G., et al. 2000, *ApJ*, 532, L55
- Menou, K, Cho, J. Y-K., Hansen, B. M. S., & Seager, S. 2002, *astro-ph/0210499*
- Perryman, M.A.C. 1997, *The Hipparcos and Tycho Catalogues* (ESA SP-1200, Noordwijk:ESA)
- Saumon, D., Chabrier, G., and Van Horn, H. 1995, *ApJS*, 99, 713
- Seager, S. & Sasselov, D. D. 2000, *ApJ*, 537, 916
- Seager, S. and Mallén-Ornelas, G. 2003, *ApJ*, 585, 1038
- Showman, A. P. & Guillot, T. 2002, *A&A*, 385, 166
- Sudarsky, D., Burrows, A., & Pinto, P. 2000, *ApJ*, 538, 885
- Sudarsky, D., Burrows, A., and Hubeny, I. 2003, accepted to *ApJ*
- Zapolsky, H.S. and Salpeter, E.E. 1969, *ApJ*, 158, 809

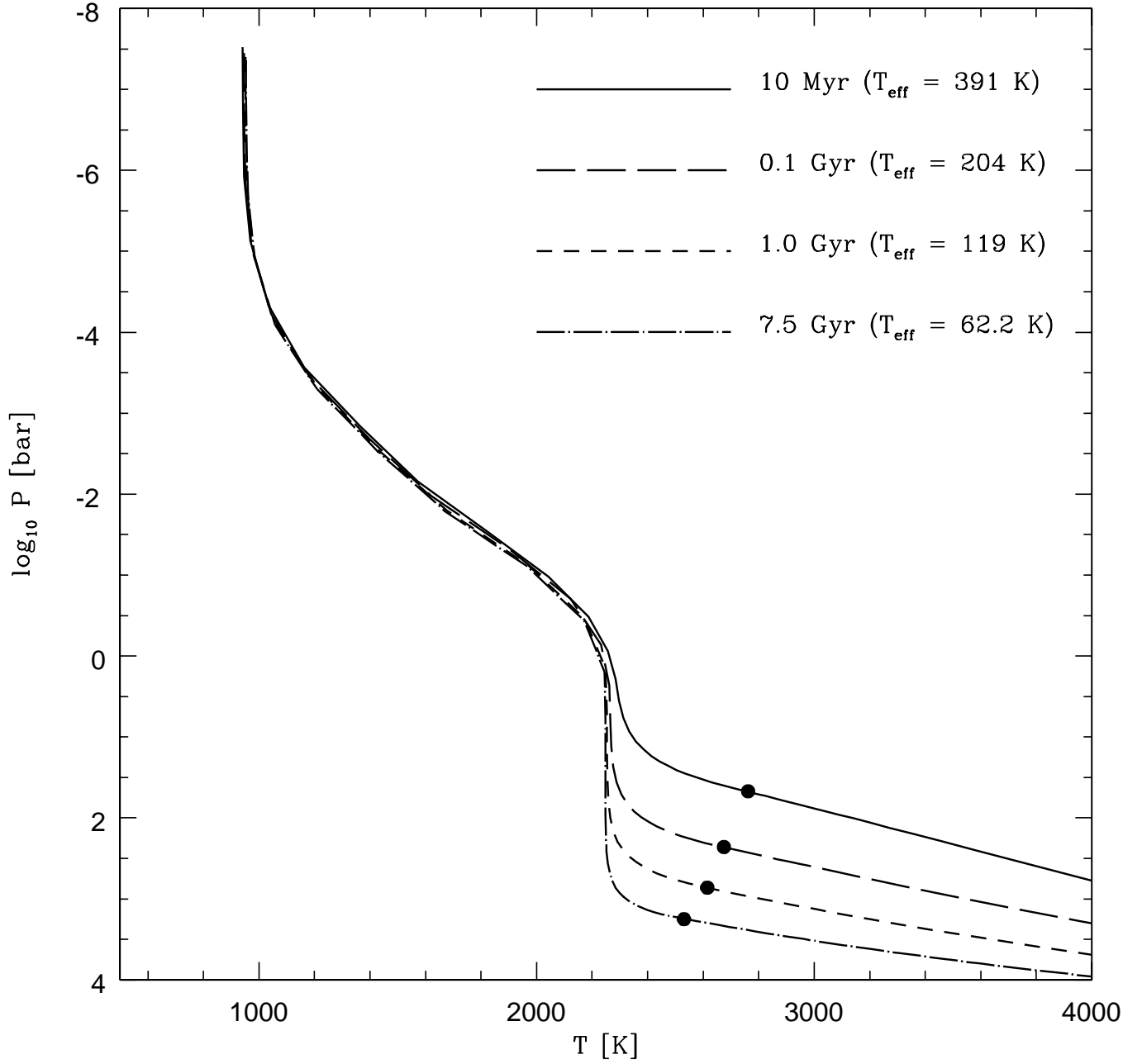


FIG. 1.— Temperature (in Kelvin) versus pressure (in bars) profiles along the evolutionary track of the model depicted in solid blue on Fig. 2. The parameters for that curve are $f = 0.5$ and $Y_{\text{He}} = 0.30$ and the TiO/VO opacity at depth has been dropped. The large dots indicate the positions of the radiative-convective boundary. The solid curve is at an age of 10 Myr and has a T_{eff} (inner boundary flux) of 391 K, the long dashed curve is at 0.1 Gyr and has a T_{eff} of 204 K, the short dashed curve is at 1.0 Gyr and has a T_{eff} of 119 K, and the dot-dashed curve is at 7.5 Gyr and has a T_{eff} of 62.2 K. See Fig. 2 and the text for details.

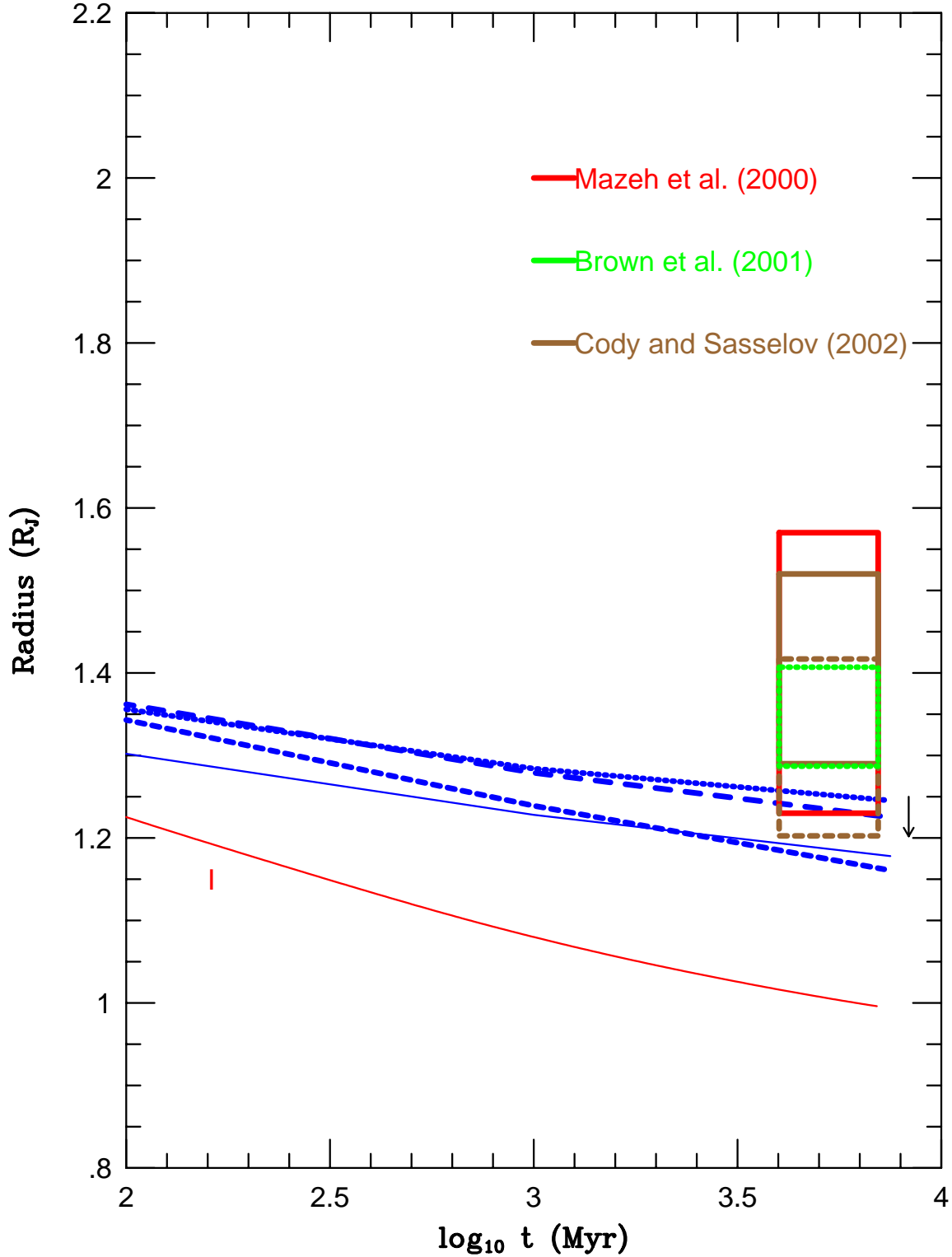


FIG. 2.— Theoretical evolutionary trajectories (blue) of the radii of HD 209458b (in R_J ; 7.149×10^4 km) with age (in Myrs). Model I (solid) is for a $0.69 M_J$ object in isolation (Burrows et al. 1997). The $\pm 1 - \sigma$ error boxes for the inferred transit radii from Mazeh et al. (2000), Brown et al. (2001), and Cody and Sasselov (2002) are shown in red, green, and gold, respectively. The solid gold box assumes a stellar radius of $1.18 R_\odot$, while the dashed gold box assumes a stellar radius of $1.10 R_\odot$. The solid blue curve is for $f = 0.5$, $Y_{He} = 0.30$, does not include TiO/VO opacity at depth, and does not have clouds (see Fig. 1). The short dashed blue curve is similar, but includes both TiO/VO opacity and a forsterite cloud at altitude (Fortney et al. 2003). The dotted blue curve is for $f = 1.0$, but otherwise has the same parameters as the solid blue curve, and the long-dashed blue curve has no TiO or VO at depth, no cloud, and a helium fraction of 0.25. The short arrow to the right of the error boxes depicts the magnitude of the radius decrease for each 10 Earth-mass increase in the mass of a possible rocky core, all else being equal. See text for details.